

**Eco-Engineered Electrospun La/Rb-MOF/Chitosan-PCL Nanofibrous
Membrane for High-Performance, Recyclable, and Sustainable Cr(VI)
Removal from Water**

Table S1. Chemical name, formula, and company

Chemical name	Formula	Company
Chitosan	C ₅₆ H ₁₀₃ N ₉ O ₃	Sigma-Aldrich, Germany
polycaprolactone	(C ₆ H ₁₀ O ₂) _n	Sigma-Aldrich, Germany
Lanthanum nitrate hexahydrate	La(NO ₃) ₃ .6H ₂ O	Sigma-Aldrich, Germany
Rubidium chloride	RbCl	Sigma-Aldrich, Germany
benzene-1,3,5-tricarboxylic acid	C ₆ H ₃ (CO ₂ H) ₃	Sigma-Aldrich, Germany
Methanol	CH ₃ OH	LOBA CHEMIE PVT.LTD, India
Ethanol	C ₂ H ₆ O	Sigma-Aldrich, Germany
Sodium hydroxide (99%, AR)	NaOH	Chimmed, Russia
Hydrochloric acid (37%, AR)	HCl	LOBA CHEMIE PVT.LTD, India

Table S2. Instruments and equipments.

Test name	Abbrevation	Instrument name	Company	Illustration
Fourier transformer infrared	FT-IR	A Nicolet IS10 Fourier transform infrared (FTIR) spectrometer	Thermo Fisher Scientific, Waltham, MA, USA	equipped with an attenuated total reflectance accessory and which ran in the 4000-400 cm^{-1} range was used to gather FTIR spectra
Powered X-ray diffraction	PXRD	Siemens diffractometer (model D500, Germany)	Germany	patterns were captured from powder samples through the use of a Siemens diffractometer (model D500, Germany) that was fitted with a Cu-K radiation source (wavelength 1.54 Angstroms (\AA)) operating at 30 kV and 20 mA.
Scanning Electron Microscope	SEM	(JSM-6510LV, JEOL Ltd., Tokyo, Japan)	JEOL Ltd., Tokyo, Japan	The morphology of the investigated sorbents was analyzed with the use of a scanning electron microscope
X-ray photoelectron spectroscopy	XPS	K-ALPHA (Themo Fisher Scientific, USA)	Themo Fisher Scientific, USA	Used for determination the elemental analysis for the compound
Braunnar Emmet Teller	BET	Quantachrome Instruments, Anton Paar Quanta Tec, Inc., Boynton Beach, FL, USA	Quanta Tec, Inc., Boynton Beach, FL, USA	was utilised for surface and pore analysis (Brunauer Emmett-Teller (BET) surface area, porous volume, and pore size), and NovaWin Software (v11.0) was used for data interpretation.

		USA		The BET surface area of material adsorbents was obtained by the application of nitrogen adsorption-desorption isotherms at 77K through the use of a specific analyser (Quadasorb-EVO, Quantachrome, USA).
UV-visible spectrophotometer	UV spectrophotometer	HACH LANGE DR5000	HACH LANGE Germany	Measuring the concentration of the adsorbate solution via using bear lambert law
Energy Dispersive X-ray	EDX	Leo1430VP microscope	Carl Zeiss AG, Jena, Germany	Elemntal analysis of the material
Transmission electron microscopy	TEM	TEM, FEI Teanci G2 F20, USA	FEI Teanci G2 F20, USA	Determination the morphology of the material and size
pH meter	pH	HANNA (model 211)	USA	Measuring the acidity or basicity of the solution
Sonication	Ultrasonic	Elmasonic P300H ultrasonic bath, continuous mode, power 380 W	Elma Schmidbauer GmbH, Singen, Germany	Sonication of the material as well as used to disperse material on the solution as it decrease the particle size of the material
Water bath	Shaking	GFL Orbital Shaker 3017		
Atomic	atomic absorption spectrometer	SIMAA 6000		Determination metal concentration

Table S3. True variables, codes, and their BBD levels.

Code	Variables	-1	0	+1
A	pH	2	5	8
B	Dose (g)	0.02	0.25	0.5
C	Time (min.)	5	55.5	100

Table S4. Equations used in this work to fit the data of adsorption experiments.

Serial	Equation	Nmae	Description	Ref.
1	$q_e = \frac{q_m}{1 + K_L C_e}$	Langmuir	q_e (mg.g ⁻¹) Adsorption capacity, C_e equilibrium concentration, q_m (mg.g ⁻¹) is the monolayer saturation capacity constant and K_L (L/mg) is the Langmuir constant associated with the free adsorption energy. The favorability of the adsorption process in the Langmuir model is determined by means of the R_L dimensionless factor ($R_L = 1/(1 + k_L \cdot C_0)$) as follows: $R_L = 0$, $0 < R_L < 1$, $R_L = 1$, and $R_L > 1$ indicating irreversible, favorable, linear, and unfavorable adsorption isotherms, respectively.	[1]
2	$q_e = K_F C_e^{\frac{1}{n}}$	Freundlich	K_F Freundlich isotherm constants [(mg/g)/(mg/L) ^{1/n}], and $1/n$ represents the exponent of non-linearity (i.e., C-type, L-type, and S-type isotherms). n is the Freundlich constants, and $n < 1$ indicates poor adsorption while $n = 1-2$ and $n = 2-10$ indicate average and good adsorptions, respectively. The values of n and k_F are calculated, respectively	[2]
3	$q_e = q_m \exp(-\beta \varepsilon^2)$ $\varepsilon = RT \ln\left(1 + \frac{1}{C_e}\right)$ $E_{DR} = \sqrt{\frac{1}{2K_{DR}}}$	Dubinin–Radushkevich	q_D is the maximum monolayer adsorption capacity (mg/g), B_D is the activity coefficient related to the apparent free energy of adsorbate adsorption onto the adsorbent (mol ² /kJ ²), ε_D is the Polanyi potential which is related to the equilibrium concentration, and E is the mean adsorption energy.	[3]
4	$q_e = Q_{max} \frac{RT}{b} \ln(K_T C_e)$	Temkin	K_T is the Temkin isotherm constant or equilibrium binding constant (L/mg) corresponding to the maximum binding energy, and b_T is the Temkin isotherm constant related to the heat of adsorbate adsorption onto the adsorbent due to adsorbent-adsorbate interaction (J/mol), R is the gas constant (8.314 J/mol/K), and T is the absolute temperature (herein 298 K).	[4]

	$q_e = \frac{q_m k_T c_e}{(1 + (K_L C_e)t)1/t}$	Toth	q _e : amount of adsorbate adsorbed at equilibrium (mg/g), C _e :equilibrium concentration of adsorbate in solution (mg/L) q _{max} : theoretical maximum adsorption capacity (mg/g) K _T : Toth isotherm constant related to affinity (L/mg) t: heterogeneity parameter (dimensionless)	[5]
5	$q_t = q_e(1 - e^{-k_1 t})$	Pseudo-First-order kinetic	q_e and q_t are the adsorption capacities at equilibrium and time t (mg/g), and k_1 is the rate constant (min ⁻¹), respectively.	[6]
6	$q_t = \frac{t K_2 q_e^2}{1 + q_e K_2 t}$	Pseudo-Second-order kinetic	k_2 is the pseudo-second order constant (mg/(g.min))	[7]
7	$q_t = K_i t^{1/2} + X$	Intraparticle diffusion	q_t is the adsorption capacity at time t in (mg/g), k_{int} is the intraparticle diffusion rate constant (mg·g ⁻¹ ·min ^{-1/2}), and C is a constant related to the the thickness of the boundary layer (mg/g).	[8]
8	$q_t = \frac{1}{\beta} \ln(\alpha \beta t + 1)$	Elovich	The constants α chemical adsorption rate (mg.g ⁻¹ min ⁻¹), and β Coefficient in relation with extension of covered surface	[9]
9	$\Delta G^\circ = \Delta H^\circ - T\Delta S^\circ$	Gibbs free energy	ΔG° : Gibbs free energy change; K _d : equilibrium constant; R: gas constant; T: temperature.	[10]
10	$\ln K_d = \frac{\Delta S^\circ}{R} - \frac{\Delta H^\circ}{RT}$	Van't Hoff	ΔS° : entropy change; ΔH° : enthalpy change.	[11]
11	$\ln K_d = \ln A - \left(\frac{Ea^0}{R}\right) \frac{1}{T}$	Arhinus	Ea was the activation energy, A Arhinus constant, R ideal gas constant 8.314 J/mol K, T (K) is the absolute solution temperature	[12]

Table S5: Identification of the peaks of La 3d

La-Rb-MOF/CS-PCL			Cr@La-Rb-MOF/CS-PCL		
Bending energy	%	Identification	Bending energy	%	Identification
835.93	25.68	La 3d _{5/2} —La(III)—O (MOF lattice)	831.91	17.76	La 3d _{5/2} —La(III)—O (coordination altered after Cr adsorption)
838.36	2.34	La 3d _{5/2} —Satellite/shake-up	836.32	10.84	La 3d _{5/2} —Satellite/shake-up due to ligand/electron transfer
839	26.55	La 3d _{5/2} —La(III)—O—C (carboxylate)	840	17.23	La 3d _{5/2} —La(III)—O—C (carboxylate, chelated ligand)
846.45	22.96	La 3d _{3/2} —La(III)—O (MOF lattice)	846.21	17.16	La 3d _{3/2} —La(III)—O (coordination altered after Cr adsorption)
849.33	3.41	La 3d _{3/2} —Satellite/shake-up	850.88	15.62	La 3d _{3/2} —Satellite/shake-up due to ligand/electron transfer
851.87	15.31	La 3d _{3/2} —La(III)—O—C (chelated)	855.79	18.72	La 3d _{3/2} —La(III)—O—C (carboxylate, chelated ligand)
853.39	3.77	La 3d _{3/2} —Satellite/shake-up	856.04	2.67	La 3d _{3/2} —Satellite/shake-up due to ligand/electron transfer

Table S6. List of abbreviation.

Symbol	Definition
q_e	the adsorbed amount of dye at equilibrium concentration (mg.g ⁻¹)
q_{mL}	the maximum sorption capacity (corresponding to the saturation of the monolayer, (mg.g ⁻¹)
K_L	Langmuir binding constant which is related to the energy of sorption (L/mg)
C_e	is the equilibrium concentration of dyes in solution
K_F	Freundlich constants related to the sorption capacity (mg/g) (L/mg) ^{1/n}
n	intensity
K_{DR}	constant related to the sorption energy (mol ² k J ⁻²)
q_{DR}	theoretical saturation capacity (mg/g)
ε	Polanyi potential (J ² mol ⁻²)
R	Gas constant (8.314 J.mol ⁻¹ K ⁻¹)
T	temperature where the adsorption occurs
A_T	Temkin isotherm constant
b_T	Temkin constant in relation to heat of adsorption (J.mol ⁻¹)
q_t	is the amount of dye adsorbed (mmol.g ⁻¹)
K_1	Rate constant for Pseudo first order constant for the adsorption processes (min ⁻¹)
q_2	Maximum adsorption capacity for pseudo second order
K_2	Rate constant for Pseudo first order constant for the adsorption processes (g.mg ⁻¹ min ⁻¹)
α	Chemical adsorption rate (mg.g ⁻¹ min ⁻¹)
β	Coefficient in relation with extension of covered surface
ΔG°	Free Gibb's energy
ΔH°	Enthalpy
ΔS°	Entropy
K_c	distribution coefficient
C_{eq}	Concentration at equilibrium (mg/L)

Table S7. The parameter of the adsorption isotherm for Cr(VI) ions on La-Rb-MOF/CS-PCL

Isotherm	Value of parameters	
Langmuir	$q_m \text{ exp}$ (mg/g)	449.2
	q_m (mg/g)	451.8
	K_L (L/mg)	0.064
	R_L	0.075
	Reduced Chi-Sqr	51.37029
	Residual Sum of Squares	821.92458
	R-Square (COD)	0.99755
	R^2	0.99739
Freundlich	n	2.96
	K_F (mg/g) $(L/mg)^{1/n}$	92.66
	Reduced Chi-Sqr	902.91751
	Residual Sum of Squares	14446.68013
	R-Square (COD)	0.95689
	R^2	0.9542
Dubin–Radushkevich	Q_{DR} (mg.g ⁻¹)	387.04
	K_{DR} (mol ² k J ⁻²)	1.0234E-5
	E_a (kJ/mol)	31.4
	Reduced Chi-Sqr	2720.32832
	Residual Sum of Squares	43525.25312
	R-Square (COD)	0.87013
	R^2	0.86201
Temkin	b_T (J/mol)	25.2
	K_T (L/mol)	0.807
	Reduced Chi-Sqr	130.51897
	Residual Sum of Squares	2088.30349
	R-Square (COD)	0.99377
	R^2	0.99338
Jossens	K	35.16

	J	0.092
	Reduced Chi-Sqr	40.9289
	Residual Sum of Squares	613.93353
	R-Square (COD)	0.99817
	R ²	0.99792
Toth	q _m	528.62
	K _T (L/mg)	9.2
	t	0.844
	Reduced Chi-Sqr	37.29076
	Residual Sum of Squares	559.36138
	R-Square (COD)	0.99833
	R ²	0.99811

Table S8: Models of adsorption kinetic parameters of Cr(VI)ions on La-Rb-MOF/CS-PCL.

Model	Value of parameters	
Pseudo-First-order kinetic	K ₁ (min ⁻¹)x10 ⁻²	0.969
	Reduced Chi-Sqr	15.16423
	Residual Sum of Squares	288.12032
	R-Square (COD)	0.99921
	R ²	0.99916
Pseudo-second-order kinetic	K ₂ (g mg ⁻¹ min ⁻¹)x10 ⁻²	3.97E-5
	q _e (mg/g)	452.4
	Reduced Chi-Sqr	743.43356
	Residual Sum of Squares	14125.23764
	R-Square (COD)	0.96629
	R ²	0.96452
Intraparticle diffusion	K _i (mgg ⁻¹ min ^{1/2})	48.72
	X (mg/g)	68.6

	Reduced Chi-Sqr	461.41148
	Residual Sum of Squares	460950.06723
	R-Square (COD)	0.96461
	R^2	0.96461
Elovich	β (g/mg)	142.05
	α (mgg ⁻¹ .min ⁻¹)	0.00179
	Reduced Chi-Sqr	148.89259
	Residual Sum of Squares	2828.95928
	R-Square (COD)	0.9922
	R^2	0.99179
Experimental data	q _e (exp) (mmol/g)	453.6

Table S9: The thermodynamic parameters.

T (K)	ΔG° (kJ/mol)	ΔH° (kJ/mol)	ΔS° (J/mol.K)
293	-0.5582		
298	-2.11708	90.8	311.75
303	-3.67595		
308	-5.23483		
313	-6.7937		
318	-8.35258		

Table S10: Analyzing similar adsorbents for the absorption of Cr(VI) ions.

Adsorbent	Adsorption capacity (mg/g)	Initial Cr(VI) Conc. (mg/L)	Dosage (g/L)	Contact Time (min)	Ref.
3D hierarchical GO-NiFe LDH	53.6	50	1	60	[13]
NiFe-LDHs	26.78	25	1	120	[14]
Fe ₃ O ₄ /GO composite	32.3	50	2	150	[15]
mFeOOH@AC	27.2	100	1	60	[16]
α -FeOOH/carbon microspheres	55.4	20	1	30	[17]
NiO nanosheets	49	25	1	100	[18]
Two-dimensional (2D) Ti ₃ C ₂ Tx	104	50	0.5	120	[19]
Polyethyleneimine	243.7	100	0.25	60	[20]
Cu _{0.1} Ni _{0.05} O-MX	321.02	100	0.2	120	[21]
NH ₂ -Ag-MOF@CSC composite sponge	382.9	50	1	120	[22]
La-Rb/CS/PCL	449.5	400	0.8	100	This search

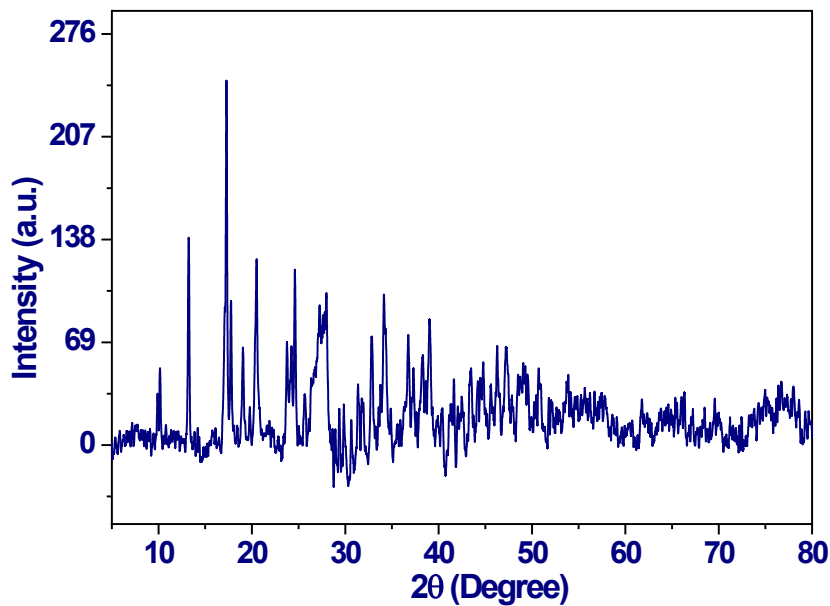


Fig.S1: XRD of La-Rb-MOF

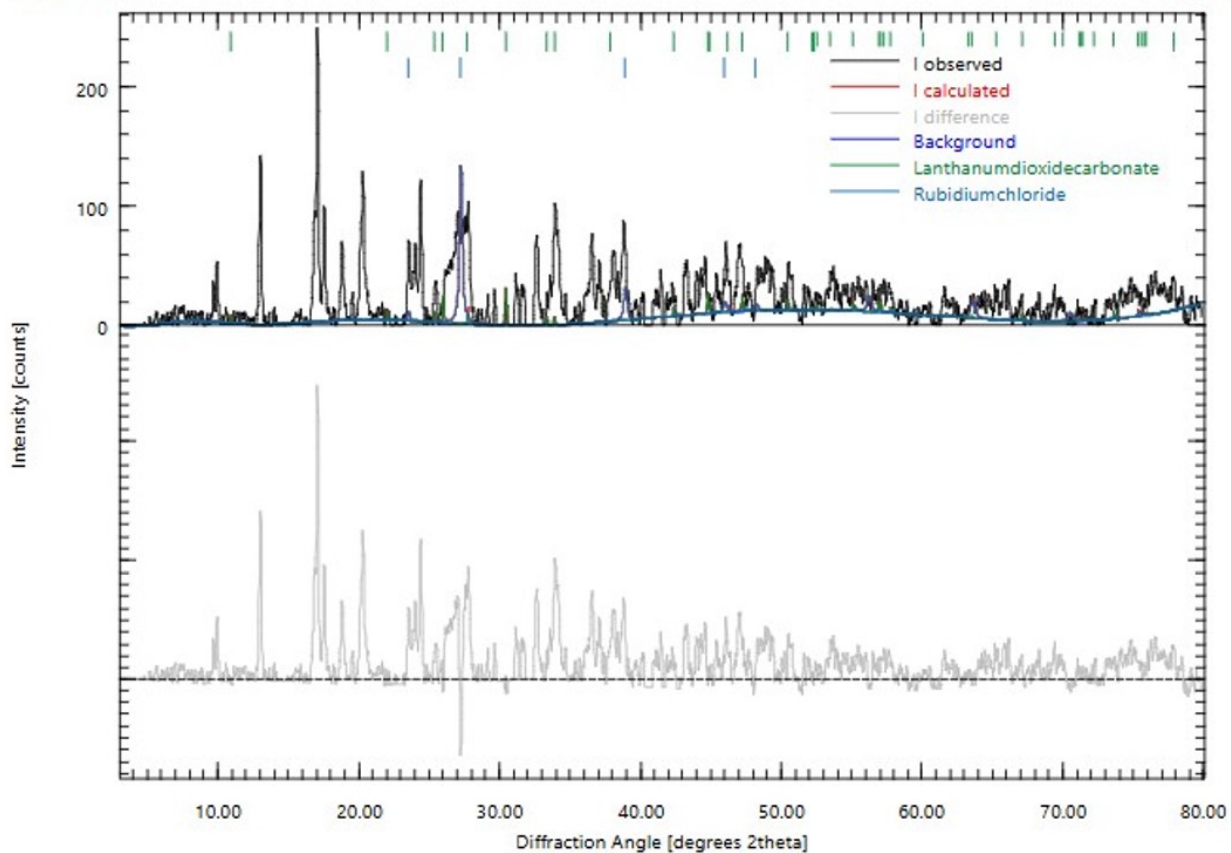


Fig.S2: Powder X-ray Diffraction Pattern and Pawley/Le Bail Refinement Comparison for La-Rb MOF: Experimental versus Simulated Profiles with Phase Assignment

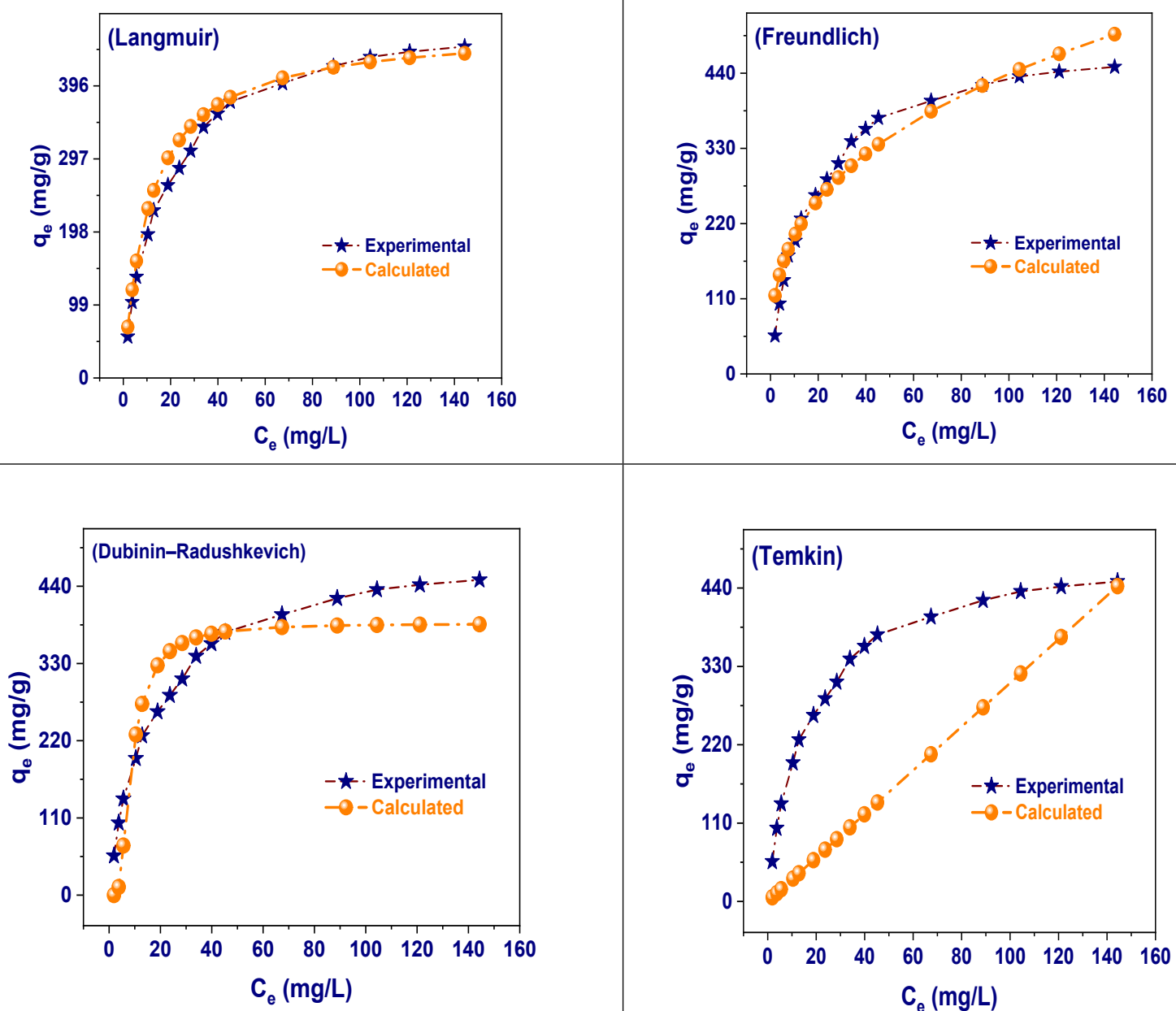


Fig. S3: Adsorption capacity of adsorption isotherm models experimental and calculated

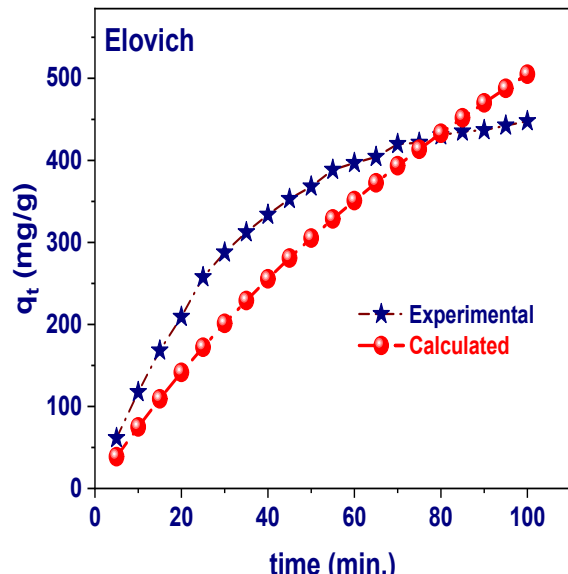
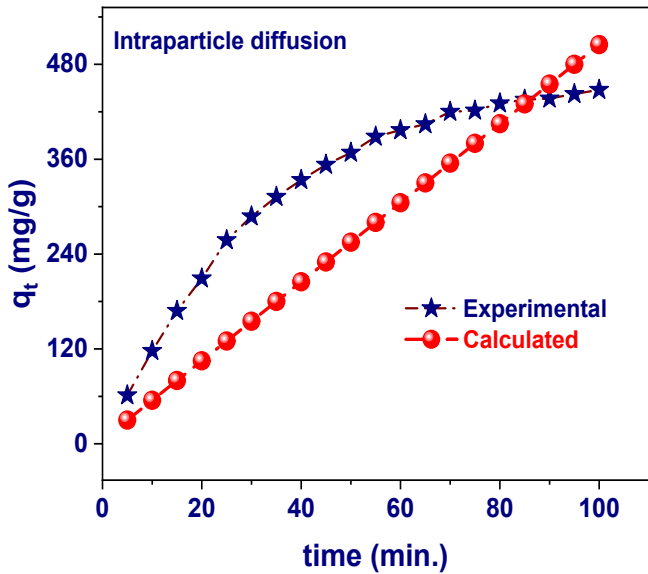
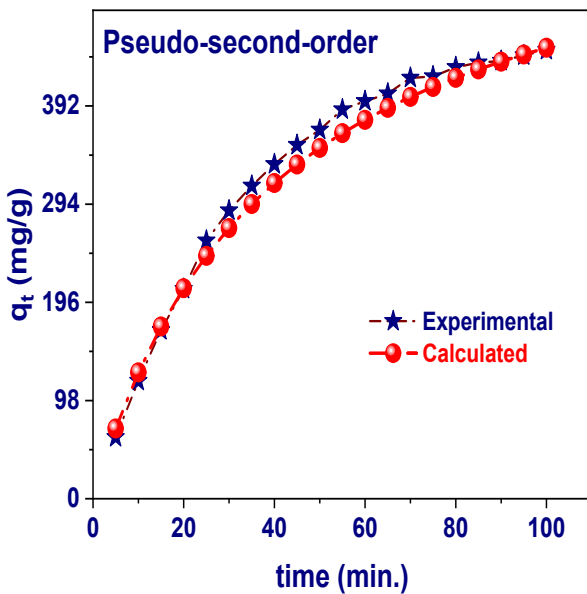
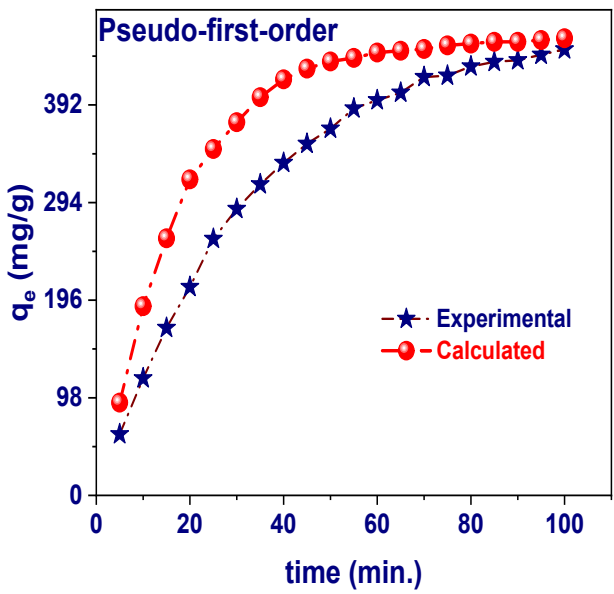


Fig. S4: Adsorption capacity of adsorption kinetic models experimental and calculated

References

- [1] I. Langmuir, The constitution and fundamental properties of solids and liquids. Part I. Solids, *J. Am. Chem. Soc.*, 38 (1916) 2221-2295.
- [2] H.M.F. Freundlich, Over the adsorption in solution, *J. Phys. Chem.*, 57 (1906) 385-471.
- [3] M. Dubinin, The equation of the characteristic curve of activated charcoal, *Proc. Acad. Sci. USSR Phys. Chem. Sect.*, 55 (1947) 327-329.
- [4] V.P. M.I. Tempkin, Kinetics of ammonia synthesis on promoted iron catalyst, *Acta Phys. Chim. USSR*, 12 (1940) 327-356.
- [5] D.P. Vargas, L. Giraldo, J.C. Moreno-Piraján, CO₂ adsorption on activated carbon honeycomb-monoliths: a comparison of Langmuir and Toth models, *International journal of molecular sciences*, 13 (2012) 8388-8397.
- [6] S.K. Lagergren, About the theory of so-called adsorption of soluble substances, *Sven. Vetenskapsakad. Handingar*, 24 (1898) 1-39.
- [7] Y.-S. Ho, G. McKay, Sorption of dye from aqueous solution by peat, *Chemical engineering journal*, 70 (1998) 115-124.
- [8] W.J. Weber Jr, J.C. Morris, Kinetics of adsorption on carbon from solution, *J. Sanit. Eng. Div.*, 89 (1963) 31-59.
- [9] M.H. Dehghani, A. Dehghan, A. Najafpoor, Removing Reactive Red 120 and 196 using chitosan/zeolite composite from aqueous solutions: Kinetics, isotherms, and process optimization, *Journal of Industrial and Engineering Chemistry*, 51 (2017) 185-195.
- [10] E.C. Lima, A. Hosseini-Bandegharaei, J.C. Moreno-Piraján, I. Anastopoulos, A critical review of the estimation of the thermodynamic parameters on adsorption equilibria. Wrong use of equilibrium constant in the Van't Hoof equation for calculation of thermodynamic parameters of adsorption, *Journal of molecular liquids*, 273 (2019) 425-434.
- [11] H.N. Tran, S.-J. You, A. Hosseini-Bandegharaei, H.-P. Chao, Mistakes and inconsistencies regarding adsorption of contaminants from aqueous solutions: a critical review, *Water research*, 120 (2017) 88-116.
- [12] B. Oladipo, E. Govender-Opitz, T.V. Ojumu, Kinetics, thermodynamics, and mechanism of Cu (II) ion sorption by biogenic iron precipitate: using the lens of wastewater treatment to diagnose a typical biohydrometallurgical problem, *ACS omega*, 6 (2021) 27984-27993.
- [13] Y. Zheng, B. Cheng, W. You, J. Yu, W. Ho, 3D hierarchical graphene oxide-NiFe LDH composite with enhanced adsorption affinity to Congo red, methyl orange and Cr (VI) ions, *Journal of hazardous materials*, 369 (2019) 214-225.
- [14] Y. Lu, B. Jiang, L. Fang, F. Ling, J. Gao, F. Wu, X. Zhang, High performance NiFe layered double hydroxide for methyl orange dye and Cr (VI) adsorption, *J Chemosphere*, 152 (2016) 415-422.
- [15] M. Liu, T. Wen, X. Wu, C. Chen, J. Hu, J. Li, X. Wang, Synthesis of porous Fe 3 O 4 hollow microspheres/graphene oxide composite for Cr (VI) removal, *J Dalton Transactions*, 42 (2013) 14710-14717.
- [16] M. Su, Y. Fang, B. Li, W. Yin, J. Gu, H. Liang, P. Li, J. Wu, Enhanced hexavalent chromium removal by activated carbon modified with micro-sized goethite using a facile impregnation method, *J Science of the total environment*, 647 (2019) 47-56.
- [17] L. Zhang, F. Fu, B. Tang, Adsorption and redox conversion behaviors of Cr (VI) on goethite/carbon microspheres and akaganeite/carbon microspheres composites, *J Chemical Engineering Journal*, 356 (2019) 151-160.
- [18] J. Zhao, Y. Tan, K. Su, J. Zhao, C. Yang, L. Sang, H. Lu, J. Chen, A facile homogeneous precipitation synthesis of NiO nanosheets and their applications in water treatment, *J Applied Surface Science*, 337 (2015) 111-117.

[19] P. Karthikeyan, K. Ramkumar, K. Pandi, A. Fayyaz, S. Meenakshi, C.M. Park, Effective removal of Cr (VI) and methyl orange from the aqueous environment using two-dimensional (2D) Ti₃C₂Tx MXene nanosheets, *J Ceramics International*, 47 (2021) 3692-3698.

[20] Z. Wu, C. Zhao, W. Zeng, X. Wang, C. Liu, Z. Yu, J. Zhang, Z. Qiu, Ultra-high selective removal of CR and Cr (VI) from aqueous solutions using polyethyleneimine functionalized magnetic hydrochar: Application strategy and mechanisms insight, *J Chemical Engineering Journal*, 448 (2022) 137464.

[21] S. Adil, J.-O. Kim, Enhanced adsorption performance of a Cu/Ni-MXene composite for phosphate recovery and removal of Cr (VI) from aqueous solutions, *J Separation Purification Technology*, 326 (2023) 124725.

[22] A.M. Alsuhaimi, A.A. Alayyafi, L.A. Albedair, M.G. El-Desouky, A.A. El-Binary, Efficient fabrication of a composite sponge for Cr (VI) removal via citric acid cross-linking of metal-organic framework and chitosan: adsorption isotherm, kinetic studies, and optimization using Box-Behnken design, *Materials Today Sustainability*, 26 (2024) 100732.